INTERNATIONAL JOURNAL FOR NUMERICAL METHODS IN FLUIDS
Int. J. Numer. Meth. Fluids 2002; **39**:821–841 (DOI: 10.1002/fld.331)

A rationale for implicit turbulence modelling★

Len G. Margolin*,† and William J. Rider‡

Los Alamos National Laboratory, Los Alamos, NM 87545, U.S.A.

SUMMARY

We present a rationale for the success of nonoscillatory finite volume (NFV) difference schemes in modelling turbulent flows without need of subgrid scale models. Our exposition focuses on certain truncation terms that appear in the modified equation of one particular NFV scheme, MPDATA. We demonstrate that these truncation terms have physical justification, representing the modifications to the governing equations that arise when one considers the motion of finite volumes of fluid over finite intervals of time. Published in 2002 by John Wiley & Sons, Ltd.

KEY WORDS: turbulence; large eddy simulation; Burgers' equation

1. INTRODUCTION

Recently, a class of finite difference methods has exhibited the remarkable property of producing large eddy simulations (LES) of turbulent flow without recourse to any explicit subgrid scale model [1–3]. These, the nonoscillatory finite volume (NFV) schemes, so far are the only class of schemes to demonstrate this property, which we term implicit turbulence modelling.

The goal of this paper is to provide a rationale for the implicit turbulence modelling ability of the NFV schemes. It is clear that the effects of the unresolved scales of motion are modelled by the propitious form of the truncation error of the numerical approximations. Our approach here will be to analyse the numerical scheme through its modified equation—the PDE that the algorithm more closely approximates including the most important truncation terms. We will perform this analysis in the context of Burgers' equation in one dimension. It will be clear that the issues lie in the treatment of the advective terms, and that the derivation can be readily extended to more dimensions, and to other equations.

★This work performed under the auspices of the U.S. Department of Energy by Los Alamos National Laboratory under Contract W-7405-ENG-36. This article is a U.S. Government work and is in the public domain in the U.S.A.

*Correspondence to: L. Margolin, Center for Nonlinear Studies, Los Alamos National Laboratory, Los Alamos, New Mexico 87545, U.S.A.
†Center for Nonlinear Studies, MS B258. E-mail: len@lanl.gov
‡Computer and Computational Sciences Division, MS D413. E-mail: wjr@lanl.gov

Received October 2001
Published in 2002 by John Wiley & Sons, Ltd. *Revised December 2001*

We will begin our investigation in Section 2 by analysing the specific NFV scheme MPDATA [4, 5] applied to Burgers' equation. We will construct its modified equation, keeping terms up to the third order in space and time. MPDATA in particular is second-order accurate, meaning that its largest truncation error is of third order. We will focus on a particular third-order truncation term, the product of a first-order and a second-order spatial derivative—$u_x u_{xx}$. We refer to this as the nonlinearly dispersive term. Qualitatively, terms with similar form appear in other physical theories. For example, terms of this general form are derived to regularize momentum transfer in shocked flows [6]. Perhaps of more relevance, terms of this form also appear in several turbulence models [7–9], and in particular in a newly proposed large-eddy theory known as α-models [10, 11]. We will briefly review these theories and models in Section 3.

Such associations are suggestive, but hardly sufficient to serve as a compelling rationale for using NFV schemes for implicit turbulence modelling. Indeed, one might suspect that a more fundamental principle underlies all of these theories and could provide a unifying perspective. One common feature of many (if not all) of these theories is that they apply to finite volumes of the fluid. This recognition has led us to consider the difference between the governing equations of an infinitesimal point of fluid and a finite volume of fluid. The equations governing a finite volume of fluid are derived from the point equations, but are different due to the nonlinearity of the advective terms in the latter—a fact that has been long appreciated by theorists and modellers studying turbulence. What is unexpected is that a straightforward and justifiable derivation of the finite volume equations leads directly to nonlinearly dispersive terms.

Details and discussion of this derivation will be given in Section 4. Here we preview the main conclusion of this paper. If the modified equation of the numerical scheme is compared to the point equations, one would identify the nonlinearly dispersive terms as truncation error. However, since we are approximating the evolution of a finite volume (i.e., a computational cell), it is more appropriate to compare the modified equation to the (analytic) finite volume equations derived in Section 4; then we realize that these terms are not numerical error, but legitimately describe the physics. We conclude that *the success of NFV schemes is a reflection of their more accurate approximation of the governing equations for the motion of a finite volume of fluid and the associated entropy production.*

We have been careful to emphasize the qualitative nature of the appearance of the nonlinearly dispersive terms. There is no *a priori* reason to believe that the dimensionless coefficients of these terms in the numerical algorithm are 'correct'—perhaps optimal is a better word. Departing here from our analytic approach, we have constructed a model for simulating Burgers' equation using fourth-order accurate Runge–Kutta methods. To this algorithm, we can explicitly add various third-order terms, separately or in combination, and with arbitrary coefficients.

Our main application of this model will be to validate the use of the modified equation as a continuous proxy of the numerical algorithm. As the modified equation is based on Taylor series expansion, one might be concerned that the series is not convergent at the shortest resolved wavelengths and so not relevant. In Section 6, we will use our high-order Burgers' model to explicitly address this concern. In particular, we will compare a simulation using MPDATA to an equivalent simulation of its modified equation; the correspondence of the two calculations lends credence to our approach. We will also use our model to evaluate the importance of the truncation error terms that do not have a physical analogue.

2. MPDATA

Our goal in this section is to provide a brief introduction to the NFV scheme MPDATA, and to the derivation of its modified equation. MPDATA (Multidimensional Positive Definite Advection Transport Algorithm) is a particular example of an NFV scheme. We emphasize that implicit turbulence modelling is not a unique property of MPDATA, but is shared by many (if not all) NFV schemes. We have chosen to use MPDATA as our paradigm partly because it is amenable to analysis and partly because of our own familiarity with this scheme. A complete review of MPDATA including its properties and its many options can be found in Reference [4].

By nonoscillatory, we identify properties such as sign preservation or monotonicity preservation. These properties have great practical importance in numerical simulations, since they are closely connected [12] to the second law of thermodynamics. In particular, nonoscillatory schemes, with suitable restrictions on the computational time step, are nonlinearly stable. In general, these methods have adaptive finite difference stencils and are nonlinear even for linear equations. By finite volume, we single out those schemes written in flux form, as opposed to advective form. Flux form schemes estimate the advective terms as the sum of fluxes entering and leaving a volume (i.e., computational cell), rather than estimating these terms at a single point. Because of detailed balance—that the flux into a cell is exactly the negative of the flux leaving its neighbour—flux form schemes are conservative to the level of numerical roundoff error.

Although most NFV scheme are based on the idea of flux limiting, MPDATA is formulated more directly on the iterated properties of upstream differencing. In its most basic form, MPDATA is sign preserving (but not monotonicity preserving), and second-order accurate. MPDATA is a two-time level algorithm. It is a multidimensional scheme, and its implementation does not involve spatial splitting.

A basic tool in developing MPDATA is Taylor series analysis, leading to the concept of the modified equation. Here we describe the derivation of the basic MPDATA algorithm to simulate the simple case of one-dimensional advection of a scalar $\psi(x,t)$ by a constant velocity field a.

$$\psi_t = -a\psi_x \tag{1}$$

The first step is a upwind donor cell scheme; the scheme depends on the sign of the velocity

$$\psi_j^{n+1} = \psi_j^n - (f_{j+\frac{1}{2}} - f_{j-\frac{1}{2}}) \tag{2}$$

where the flux is:

$$f_{j+\frac{1}{2}} = \frac{A}{2}(\psi_j^n + \psi_{j+1}^n) - \frac{|A|}{2}(\psi_{j+1}^n - \psi_j^n) \tag{3}$$

In common notation, the subscript j identifies the computational cell, the superscript n the time, and $A = [(a\delta t)/(\delta x)]$ is the Courant number. Here δx is the cell width, and δt is the time step. Note that the flux (i.e., the spatial derivative) has been estimated one-half cell upstream, where the upstream direction is determined by the sign of a.

Equations (2) and (3) are stable and sign preserving when the Courant number is bounded: $A \in [-1, 1]$. However these schemes are only first-order accurate. That is, expanding the

discrete field ψ_j^n in a Taylor series as if it were a continuous function, we find that Equations (2) and (3) more accurately approximate the advection-diffusion equation

$$\psi_t = -a\psi_x + \partial_x(K\psi_x) \tag{4}$$

where the diffusion coefficient $K = [(\delta x^2)/(2\delta t)](|A| - A^2)$. Under the assumed bounds on the Courant number, the diffusion coefficient K is positive thus insuring stability. We say the scheme is first-order accurate, meaning that the error is of order $\mathcal{O}(\delta x^2)$ relative to ψ itself. We refer to Equation (4) as the modified equation of Equations (2) and (3).

To derive a more accurate algorithm, one can compensate the second-order (i.e., diffusional) error, by estimating the error and subtracting it in the algorithm. The essence of MPDATA is how we estimate that error; to preserve the nonoscillatory properties of the solution, we use an upstream estimate of the error. We write the error term in advective form

$$\partial_x(K\partial_x\psi) \simeq \partial_x(a^{(1)}\psi) \tag{5}$$

where

$$a^{(1)} \equiv \frac{\delta x^2}{2\delta t}(|A| - A^2)\frac{1}{\psi}\partial_x\psi \tag{6}$$

is called a pseudo velocity. To complete the basic MPDATA algorithm, we now do a second step, repeating Equation (2) using the pseudo velocity in Equation (3). Note that if ψ_j is defined at the centres of computational cells, then the pseudo velocity is defined at the cell edges halfway between the cell centres, and varies in space and time even though a is constant. It is easy to show that the bounds on the physical Courant number imply the same bounds on the pseudo velocity. Each step of the algorithm is stable and sign-preserving and therefore the overall scheme also has these properties. The error terms in the modified equation of basic MPDATA (not shown) now appear at the third order, implying that MPDATA is a second-order algorithm.

The extension of the MPDATA algorithm to Burgers' equation

$$u_t = -uu_x + \lambda u_{xx} \tag{7}$$

where u is the fluid velocity and λ is the viscous diffusivity, is straightforward; details of this extension are discussed in Reference [4]. The derivation of its modified equation is most easily done using computer manipulation tools; we present the modified equation here without derivation. To facilitate comparison with our analytic results, we denote the solution of the MPDATA algorithm by $\bar{u}$ as the cell-averaged velocity.

$$\bar{u}_t = -\bar{u}\bar{u}_x + \lambda\bar{u}_{xx} + \lambda\left(\frac{\bar{u}_{xxtt}(\delta t)^2}{8} + \frac{\bar{u}_{xxxx}(\delta x)^2}{12}\right) + \left(\frac{|U|}{4} - \frac{1}{6}\right)\bar{u}\bar{u}_{xxx}(\delta x)^2$$

$$+\frac{(1-|U|)(\delta x)^2}{4}(|\bar{u}_x|\bar{u}_{xx} - \bar{u}_x\bar{u}_{xx}) - \frac{\delta t\delta x}{4}(sgn(U)|\bar{u}_x|(\bar{u}_x)^2 - U(\bar{u}_x)^3) + \cdots \tag{8}$$

Here $U \equiv \frac{\bar{u}\delta t}{\delta x}$ and $sgn(U) \equiv \frac{|U|}{U}$. We note that some of the dimensionless coefficients may change depending on the details of the implementation of MPDATA. We have assumed that the diffusive term is centered in time—see Section 3.3 in Reference [4].

The MPDATA algorithm for Burgers' equation depends on both the sign of $\bar{u}$ and the sign of $\bar{u}_x$. Equation (8) unifies the four combinations that can occur generally in a single formula. We add that this equation also describes the situation when the advective velocity changes sign across the cell. However, it is not valid for those cells where the gradient of the velocity changes sign across the cell. In these cells, which represent local minima or maxima of the velocity field, MPDATA becomes only first-order accurate.

3. PHYSICAL THEORIES AND COMPUTATIONAL MODELS

The goal of this section is to point out the resemblance of our results to previous work, both theoretical and computational. First we will briefly review a variety of results. Then we will discuss in more detail a recently proposed set of equations for turbulent flows, generically named the Navier–Stokes alpha model (α-model). We will see that the theoretical and computational models are very similar in form, but with one essential difference: The computational models are strictly dissipative while the theoretical models are not. In the end, the difference is whether the model is locally as well as globally dissipative. Our results follow this pattern as well, and we will offer some discussion in Section 5. With regard to the α-model, we will show that the equations are very similar to our analytic results in Section 4; however the derivation, the assumptions and even the interpretation of the equations are very different.

3.1. Survey of theories and models

Let us begin by noting that the presence of the nonlinear term $-u_x u_{xx}$ in the right-hand-side of the momentum equation leads to $(u_x)^3$ in the associated energy equation (see Section 5). This term is dissipative in compression, but not in expansion. On the other hand, the nonlinear term $|u_x|u_{xx}$ leads to $-|(u_x)^3|$, which is always dissipative.

On the theoretical side, Bethe [13] showed that the rate of entropy production across a shock is

$$T\frac{\partial S}{\partial t} = -\frac{\mathscr{G}}{12c_s}(\Delta u)^3 \tag{9}$$

where S is the entropy, T is the temperature, c_s is the sound speed and $\mathscr{G}$ is the fundamental thermodynamic derivative $\frac{\partial^2 p}{\partial V^2}$. Note that this expression increases entropy in compression, but decreases in expansion.

In hydrodynamic turbulence, Kolmogorov [14] has derived a remarkably similar form

$$-\overline{\frac{\partial K}{\partial t}}\mathscr{L} = \overline{\frac{\partial S}{\partial t}}\mathscr{L} = -\frac{5}{4}\overline{(\Delta u)^3} \tag{10}$$

where K is the kinetic energy, and the bar indicates spatial averaging over the length $\mathscr{L}$. Frisch [15] has derived a similar formula for the regularization of shocks in a Burgers fluid

$$\overline{\frac{\partial K}{\partial t}}\mathscr{L} = \frac{1}{12}\overline{(\Delta u)^3} \tag{11}$$

As in Bethe's formula, the entropy is increased in compression in each of these formulas, but decreases in expansion.

In the field of computational fluid dynamics, it has been known for more than 50 years that direct simulation of the compressible Navier–Stokes equations for high speed flows with shocks leads to unphysical oscillations. In a seminal paper, Von Neumann and Richtmyer [6] attributed these oscillations to the lack of sufficient entropy production in the shock, and suggested adding an artificial viscosity to augment the pressure in the momentum and energy equations. The artificial viscosity, which is added to the physical pressure, has the one-dimensional form:

$$q = -c\delta x^2 u_x |u_x| \tag{12}$$

where δx is the computational cell size and c is a dimensionless constant of order unity. Note that it is the gradient of q that enters the momentum equation. The absolute value sign guarantees energy dissipation and entropy production. In modern shock wave codes, the viscosity usually is turned off in expansion altogether.

For numerical applications to turbulent flows, Smagorinsky [7] proposed a multidimensional subgrid model for the Reynolds stress:

$$\tau_{ij} = -\nu_T S_{ij} \tag{13}$$

where $S_{ij} \equiv \frac{1}{2}(\frac{\partial u_i}{\partial x_j} + \frac{\partial u_j}{\partial x_i})$ and the turbulent viscosity $\nu_T \equiv (c\delta x^2 S_{ij} S_{ij})^{\frac{1}{2}}$. Here again, c is a dimensionless constant. The similarity between Equations (12) and (13) is not accidental—see References [16, 17]. Note again that the Smagorinsky model is absolutely dissipative.

Leonard [8] has proposed an expansion for the advective terms, based on the Gaussian filter. The Leonard expansion is:

$$\widehat{u u_x} \simeq \hat{u}\hat{u}_x + (\Delta)^2 \hat{u}_x \widehat{u_{xx}} + \frac{(\Delta)^4}{2!} \widehat{u_{xx}} \widehat{u_{xxx}} + \cdots \tag{14}$$

Here the top hat indicates spatial filtering over the length scale Δ. Unlike the previous computational models, this model is not absolutely dissipative. More recently, Winkelmans *et al.* [9] have discussed the Leonard model, noting that it provides significant backscatter, but not sufficient dissipation. They suggest augmenting the model with a (dynamic) Smargorinsky term to increase the dissipation of energy.

3.2. *Burgers α-model*

The α-models were introduced to describe the mean motion of ideal incompressible fluids (cf. References [10, 11] and the references therein). They are derived in an elegant Euler–Poincaré formalism, which is the Lagrangian version of the Lie–Poisson Hamiltonian framework. In the derivation one does a Reynolds decomposition of the motion of a fluid parcel along a Lagrangian trajectory. When the formalism is applied to one-dimensional Burgers equation, one derives

$$\begin{aligned} v_t &= -\partial_x \left(\bar{u} v - \frac{1}{2}(\bar{u})^2 - \frac{\alpha^2}{2}(\bar{u}_x)^2 \right) + \lambda v_{xx} \\ v &\equiv \bar{u} - \alpha^2 \bar{u}_{xx} \end{aligned} \tag{15}$$

Here the length scale α is introduced into the theory as a closure assumption concerning the correlation of fluctuating displacements, and so represents a property of the flow. Both

$\bar{u}$ and v are velocities. In applications to LES turbulence modelling v is the unfiltered (or defiltered) velocity while $\bar{u}$ is the filtered velocity. Here we identify $\bar{u}$ with the mean Eulerian velocity. Eliminating v from Equation (15), and then differentiating the resulting equation to approximate and eliminate the cross-derivative $\bar{u}_{xxt}$, we derive

$$u_t = -\bar{u}\bar{u}_x - \alpha^2 \bar{u}_x \bar{u}_{xx} + \lambda(\bar{u}_{xx} - \alpha^2 \bar{u}_{xxxx}) \tag{16}$$

This result should be compared with our own analytic result (24) in Section 4. The latter has additional terms resulting from the averaging in time and proportional to the time scale T. These same terms are missing in the Leonard model. Like the other analytic results reviewed here, the α-model is not absolutely dissipative. Thus one might suspect the need to add extra dissipation when employing the α-model for LES.

4. FINITE VOLUME EQUATIONS

In this section we derive our principal result, the equations that describe the evolution of finite volumes of Burgers fluid. First we will consider smooth (i.e., laminar) flows. Using Taylor series expansion, we will integrate Burgers' equation over a finite interval in space and time, leading to analytic equations very similar in form to the modified equations of MPDATA (8). We note that this procedure and result do not apply to turbulent flows without additional assumptions and derivation. We will then describe a physically reasonable assumption and analysis that justifies using the same volume-averaged equations for turbulent flows as for laminar flows.

In either case, we emphasize that the choice of the size of the intervals is arbitrary and in particular is not restricted by the details of the flow. In the next section, we will identify the length scale with the size of a computational cell, and the time scale with the computational timestep.

4.1. Laminar flows

We again consider a one-dimensional fluid governed at each infinitesimal point by Burgers' equation. First we will assume that the flow is smooth on the length scale L and time scale T—i.e., that all flow features are resolved on these scales. We will define such a flow as being laminar on the scales L and T. Because of the assumed smoothness, we can expand the velocity u in a local Taylor series in space and time:

$$u(x+x', t+t') = u(x,t) + u_x x' + u_t t' + u_{xx}\frac{(x')^2}{2} + u_{xt}x't' + u_{tt}\frac{(t')^2}{2} + \cdots \tag{17}$$

Then we can define an averaged (in space and time) velocity

$$\begin{aligned}\bar{u}(x,t) &\equiv \frac{1}{LT}\int_{-\frac{L}{2}}^{\frac{L}{2}}\int_{-\frac{T}{2}}^{\frac{T}{2}} u(x+x', t+t')\,\mathrm{d}x'\,\mathrm{d}t' \\ &= u(x,t) + \frac{1}{6}u_{xx}\left(\frac{L}{2}\right)^2 + \frac{1}{6}u_{tt}\left(\frac{T}{2}\right)^2 + \cdots\end{aligned} \tag{18}$$

since the odd terms integrate to zero over the symmetric interval. Now $\bar{u}(x,t)$ is a continuous function, and so its derivatives can be defined. For example,

$$\bar{u}_x = u_x + \frac{1}{6}u_{xxx}\left(\frac{L}{2}\right)^2 + \frac{1}{6}u_{xtt}\left(\frac{T}{2}\right)^2 + \cdots \tag{19}$$

Note that in general, $\bar{u}_x \neq \overline{u_x}$.

Our goal is to derive the equations that govern the evolution of $\bar{u}$. The first step is to average Burgers' equation (7) term by term. The linear terms are easily treated. For example,

$$\overline{u_t} = u_t + \frac{1}{6}u_{xxt}\left(\frac{L}{2}\right)^2 + \frac{1}{6}u_{ttt}\left(\frac{T}{2}\right)^2 + \cdots \tag{20}$$

and

$$\lambda\overline{u_{xx}} = \lambda\left(u_{xx} + \frac{1}{3}u_{xxxx}\left(\frac{L}{2}\right)^2 + \frac{1}{3}u_{xxtt}\left(\frac{T}{2}\right)^2 + \cdots\right) \tag{21}$$

A direct evaluation of the nonlinear (advective) term yields:

$$\overline{uu_x} = uu_x + \frac{1}{6}\left(\frac{L}{2}\right)^2(3u_xu_{xx} + uu_{xxx}) + \frac{1}{6}\left(\frac{T}{2}\right)^2(2u_tu_{xt} + uu_{xtt} + u_xu_{tt}) + \cdots \tag{22}$$

where we have shown all terms of $\mathcal{O}(L^2, T^2)$ or lower.

At this point, the averaged equation is still written in terms of the point velocities. The second step then is to invert the set of forward relations of which Equations (18) and (19) are two examples. When the point velocity u is smooth enough, we can invert the Taylor series, to write:

$$u(x,t) \approx \bar{u}(x,t) - \frac{1}{6}\bar{u}_{xx}\left(\frac{L}{2}\right)^2 - \frac{1}{6}\bar{u}_{tt}\left(\frac{T}{2}\right)^2 + \cdots \tag{23}$$

Higher-order terms can be easily found by differentiating this expression.

Now we substitute the inverse relations into the averaged Burgers' equation terms of Equations (20), (21) and (22) to derive [to $\mathcal{O}(L^2, T^2)$]

$$\begin{aligned}\bar{u}_t = &-\bar{u}\bar{u}_x - \frac{1}{3}\bar{u}_x\bar{u}_{xx}\left(\frac{L}{2}\right)^2 - \frac{1}{3}\bar{u}_t\bar{u}_{xt}\left(\frac{T}{2}\right)^2 \\ &+ \lambda\left[\bar{u}_{xx} + \frac{1}{6}\bar{u}_{xxxx}\left(\frac{L}{2}\right)^2 + \frac{1}{6}\bar{u}_{xxtt}\left(\frac{T}{2}\right)^2\right]\end{aligned} \tag{24}$$

which is the evolution equation for $\bar{u}$.

Finally, it is convenient to rewrite $\bar{u}_t\bar{u}_{xt}$ in terms of spatial derivatives, by using Equation (24). Neglecting terms of $\mathcal{O}(\lambda^2)$, we find

$$\bar{u}_t = -\bar{u}\bar{u}_x - \frac{1}{3}\bar{u}_x\bar{u}_{xx}\left(\frac{L}{2}\right)^2 - \frac{1}{3}(\bar{u}\bar{u}_x^3 + \bar{u}^2\bar{u}_x\bar{u}_{xx})\left(\frac{T}{2}\right)^2$$

$$+\lambda\bar{u}_{xx}+\frac{\lambda}{6}((\bar{u}_x)^2\bar{u}_{xx}+\bar{u}(\bar{u}_{xx})^2+\bar{u}\bar{u}_x\bar{u}_{xxx})\left(\frac{T}{2}\right)^2$$

$$+\lambda\left[\frac{1}{6}\bar{u}_{xxxx}\left(\frac{L}{2}\right)^2+\frac{1}{6}\bar{u}_{xxtt}\left(\frac{T}{2}\right)^2\right] \tag{25}$$

4.2. *Turbulent flows*

Let us now consider flows that are not smooth on the scales L' and T', meaning that the Taylor series (17) does not converge sufficiently rapidly. We will refer to such flows are being turbulent on the scales L' and T'. The derivation of Equation (24) cannot be justified for such turbulent flows without further assumptions; i.e., if the Taylor series expansion is inaccurate, then both the forward transformation (17) and also the inverse relation (23) are questionable, or may require keeping many higher-order terms. In the previous derivation, the connection between the average velocity $\bar{u}$ and the point velocity u was critical, since it is only the latter for which we know the governing equation. However, the result of this derivation was an equation for $\bar{u}$. Furthermore, since $\bar{u}$ is averaged in length and time, we expect that it is smoother than u. This suggests an new strategy, in which we consider a hierarchy of velocity fields, and attempt to bootstrap our results.

Let us define the velocity fields averaged over the arbitrary scales L' and T' by:

$$\bar{u}(x,t,L',T')\equiv\int_{-\frac{L'}{2}}^{\frac{L'}{2}}\int_{-\frac{T'}{2}}^{\frac{T'}{2}}u(x+x',t+t')\,\mathrm{d}x'\,\mathrm{d}t' \tag{26}$$

For brevity, we suppress the coordinate dependence, implying all functions are evaluated at (x,t) except where explicitly noted otherwise. Let us now make two assumptions: the averaged velocity $\bar{u}(L',T')$ is smooth on its own scales (L',T'), and there is some set of scales (L,T) below which the point velocity $u(x,t)$ is smooth.

The first assumption is meant to imply that we can expand $\bar{u}(L',T')$ in a Taylor series in a region somewhat bigger than (L',T'). From a computational point of view, we mean that the flow can be modelled in a numerical simulation where $\bar{u}(L',T')$ is a cell-averaged quantity whose evolution can be described by a partial differential equation. This interpretation also indicates quantitatively how convergent the Taylor series need be—the remainder of the Taylor series should be of the same order or less than the truncation error of the numerical algorithm.

From the second assumption, we infer there is some set of scales (L,T) for which the point velocity $u(x,t)$ has a sufficiently convergent Taylor series. These are the scales for which simulations are DNS. The results (24) of the previous section then apply, so that

$$\bar{u}_t(L,T)=-\bar{u}(L,T)\bar{u}_x(L,T)-\frac{1}{3}\bar{u}_x(L,T)\bar{u}_{xx}(L,T)\left(\frac{L}{2}\right)^2$$

$$-\frac{1}{6}\bar{u}_t(L,T)\bar{u}_{xt}(L,T)\left(\frac{T}{2}\right)^2+\lambda\bar{u}_{xx}(L,T) \tag{27}$$

Now let us consider the averaged velocity at twice the scales—$(2L, 2L)$.

$$\bar{u}(2L,2T) \equiv \frac{1}{4LT}\left[\int_{-L}^{0}\int_{-T}^{0} u(x+x',t+t')\,\mathrm{d}x'\,\mathrm{d}t' + \int_{0}^{L}\int_{-T}^{0} u(x+x',t+t')\,\mathrm{d}x'\,\mathrm{d}t' + \int_{-L}^{0}\int_{0}^{T} u(x+x',t+t')\,\mathrm{d}x'\,\mathrm{d}t' + \int_{0}^{L}\int_{0}^{T} u(x+x',t+t')\,\mathrm{d}x'\,\mathrm{d}t'\right] \tag{28}$$

or

$$\bar{u}(x,t,2L,2T) \approx \frac{1}{4}\left[\bar{u}\left(x-\frac{L}{2},t-\frac{T}{2},L,T\right) + \bar{u}\left(x+\frac{L}{2},t-\frac{T}{2},L,T\right) + \bar{u}\left(x-\frac{L}{2},t+\frac{T}{2},L,T\right) + \bar{u}\left(x+\frac{L}{2},t+\frac{T}{2},L,T\right)\right] \tag{29}$$

Using our first assumption, we expand $\bar{u}(x,t,2L,2T)$ in a Taylor series to write (for example):

$$\bar{u}\left(x+\frac{L}{2},t+\frac{T}{2},L,T\right) \approx \bar{u}(x,t,L,T) + \left(\frac{L}{2}\right)\bar{u}_x(L,T) + \left(\frac{T}{2}\right)\bar{u}_t(L,T) + \left(\frac{LT}{4}\right)\bar{u}_{xt}(L,T) + \frac{1}{2}\left(\frac{L}{2}\right)^2\bar{u}_{xx}(L,T) + \cdots \tag{30}$$

and similarly for the other three terms of Equation (28). Combining Equations (29) and (30) leads to:

$$\bar{u}(2L,2T) \approx \bar{u}(L,T) + \frac{1}{2}\left(\frac{L}{2}\right)^2\bar{u}_{xx}(L,T) + \frac{1}{2}\left(\frac{T}{2}\right)^2\bar{u}_{tt}(L,T) + \cdots \tag{31}$$

This is the analogue of Equation (18) in the previous section. However we have expressed $\bar{u}(2L,2T)$ in terms of $\bar{u}(L,T)$, and so avoided the issues concerning the smoothness of $u(x,t)$ on the scales $(2L,2T)$.

Next, we construct the approximate inverse relation:

$$\bar{u}(L,T) \approx \bar{u}(2L,2T) - \frac{1}{2}\left(\frac{L}{2}\right)^2\bar{u}_{xx}(2L,2T) - \frac{1}{2}\left(\frac{T}{2}\right)^2\bar{u}_{tt}(2L,2T) + \cdots \tag{32}$$

Higher-order terms again can be found by differentiating this equation.

Now we have set up the transformations between $\bar{u}(L,T)$ and $\bar{u}(2L,2T)$ and so our procedure will be to average Burgers' equation (7) over the twice-wide intervals $[-L,L]$ and $[-T,T]$, writing the results in terms of $\bar{u}(L,T)$ and its derivatives. Then we will use the inverse relations to express the results in terms of $\bar{u}(2L,2T)$ and its derivatives. Assembling the terms then yields the Burgers' equation at the scales $[2L,2T]$.

There is one subtlety in the process, which is to write each twice-wide integral as the sum of four integrals as was done in Equation (28). Each of these four integrals can now be written as a function of $\bar{u}(x \pm \frac{L}{2}, t \pm \frac{T}{2}, L, T)$. Thus, we must expand each of these terms about (x, t). We show the result of this process for the nonlinear term:

$$\begin{aligned}\overline{uu_x}(2L, 2T) \approx{}& \bar{u}(L, T)\bar{u}_x(L, T) \\ &+ \frac{1}{6}\left(\frac{L}{2}\right)^2 [3\bar{u}_x(L, T)\bar{u}_{xx}(L, T) + \bar{u}(L, T)\bar{u}_{xxx}(L, T)] \\ &+ \frac{1}{6}\left(\frac{T}{2}\right)^2 [2\bar{u}_t(L, T)\bar{u}_{xt}(L, T) + \bar{u}(L, T)\bar{u}_{xtt}(L, T) + \bar{u}_x(L, T)\bar{u}_{tt}(L, T)]\end{aligned} \tag{33}$$

Finally, substituting the inverse relations (32), we derive the following result:

$$\begin{aligned}\bar{u}_t(2L, 2T) = {}& -\bar{u}(2L, 2T)\bar{u}_x(2L, 2T) + \lambda\bar{u}_{xx}(2L, 2T) - \frac{L^2}{3}\,\bar{u}_x(2L, 2T)\bar{u}_{xx}(2L, 2T) \\ &- \frac{T^2}{6}\,\bar{u}_t(2L, 2T)\bar{u}_{xt}(2L, 2T) + \lambda\left[\frac{L^2}{6}\,\bar{u}_{xxxx}(2L, 2T) + \frac{T^2}{6}\,\bar{u}_{xxtt}(2L, 2T)\right]\end{aligned} \tag{34}$$

Note that Equation (34) is exactly the same as Equation (27), written for its own scales. Said in a different way, Equation (34) is exactly the equation we would have gotten by integrating of the point velocities $u(x, t)$, if we had not been concerned about the convergence rates of the Taylor series and the inverse approximation. It is clear now that we can repeat this process, integrating Burgers equation over the scales $[4L, 4T]$, etc. and relating the averaged terms to $\bar{u}(2L, 2T)$ and its derivatives. *We conclude that the fundamental equation* (24) *or equivalently* (25) *holds at all scales.*

In considering Equation (24) or (25), one should remember that underlying every realization of the averaged flow $\bar{u}(x, t)$, there are many possible flow fields $u(x, t)$. Some of these are smooth, some are not smooth; yet all evolve identically. This leads to two conclusions:

- the description of the flow in terms of $\bar{u}(x, t, L, T)$ depends on the scales with which it is observed. That is, L and T are scales of the observer, not of the flow,
- the unresolved scales do not play a significant role in the evolution of $\bar{u}(x, t, L, T)$.

The first conclusion distinguishes our theory from the α-model, where the length scale α is assumed to derive from the properties of the flow. In our derivation, all length and time scales must derive from the equations themselves. We have neglected such possibilities in our statement of the problem, where the only physical length scale is associated with the viscosity and so is too small to play a role in the LES simulations. More generally, physical scales may arise from the initial or boundary conditions, from the forcings, or additional coupled physical processes. Each of these would require extensions to our theory.

5. COMPARISON OF THEORY AND ALGORITHMS

The close similarity of the analytic equations (25) that govern the motion of a finite volume of 'Burgers' fluid and the modified equations of MPDATA (8) provides a convincing rationale for the success of NFV schemes in simulating unresolved turbulent fluid flow. The new terms that represent the effects of considering finite volumes of fluid, derived in the previous section, correspond to terms in the modified equation, which arise from the finite volume approximations in the algorithm. This analogy underscores the importance of using a second-order accurate algorithm; a lower-order numerical truncation error would dominate those new 'physical' terms.

A close comparison of these two equations also shows a few differences, in the values of some of the dimensionless coefficients, the appearance of a purely dispersive term $\bar{u}_{xxx}$, and also in the significant appearance of an absolute value sign in the modified equation. As to the values of the dimensionless coefficients and the dispersion, it appears that the important questions concern the sensitivity of the simulation rather than accuracy. We will defer addressing these questions to the next section. In this section, we will discuss the issues associated with the absolute value sign.

We begin by comparing the finite volume energy equations, which are derived by multiplying the momentum equation by the average velocity $\bar{u}$, and integrating by parts. For the analytic equation (25), we derive

$$\frac{1}{2}(\bar{u}^2)_t = -\partial_x\left(\bar{u}\left[\frac{\bar{u}^2}{3} + \frac{\bar{u}_x^2(1+U^2/2)}{6}\left(\frac{L}{2}\right)^2\right]\right) + \frac{\bar{u}_x^3(1+U^2/2)}{6}\left(\frac{L}{2}\right)^2 + \mathcal{O}(\lambda) \tag{35}$$

where the dimensionless quantity $U \equiv [(\bar{u}L)/(T)]$. Our notation does not imply that we believe the viscous terms $\mathcal{O}(\lambda)$ are necessarily small, but that we are only concerned with the inviscid dissipation here. Note that the term on the right-hand-side inside the derivative represents advection and does not change the global balance of energy. However the term proportional to $(u_x)^3$ does alter the global energy. Furthermore, this term may be positive or negative; in particular, in regions of expansion the large scales of motion can absorb energy from the smaller (unresolved) scales of motion. From a physical point of view, this is correct. The inverse cascade, sometimes termed stochastic backscatter, is a well understood process in turbulence and plays an important role in determining the variability of the flow. From a numerical point of view, however, the term $-u_x u_{xx}$ in the momentum equation would appear to be a negative diffusion in regions of expansion potentially leading to numerical instability.

Now let us consider the finite volume energy equation derived from the MPDATA modified equation (8). There are two cases to consider, when $\bar{u}_x > 0$ (expansion) and when $\bar{u}_x < 0$ (compression). First, in expansion:

$$\frac{1}{2}(\bar{u}^2)_t = -\partial_x\left(\bar{u}\left[\frac{\bar{u}^2}{3}\right]\right) + \left(\frac{|U|}{4} - \frac{1}{6}\right)\bar{u}^2\bar{u}_{xxx}(\delta x)^2$$
$$-\frac{|\bar{u}_x|^3(|U| - U^2)}{4}(\delta x)^2 + \mathcal{O}(\lambda) \tag{36}$$

while in compression we get added terms:

$$\frac{1}{2}(\bar{u}^2)_t = -\partial_x\left(\bar{u}\left[\frac{\bar{u}^2}{3} + \frac{\bar{u}_x^2(1-|U|)}{4}(\delta x)^2\right]\right) + \left(\frac{|U|}{4} - \frac{1}{6}\right)\bar{u}^2\bar{u}_{xxx}(\delta x)^2$$
$$- \frac{|u_x|^3(1-|U|)^2}{4}(\delta x)^2 + \mathcal{O}(\lambda) \tag{37}$$

The modified equations of MPDATA (and other NFV schemes) have a coefficient of zero for the $\bar{u}_x\bar{u}_{xx}$ term in regions of expansion in contrast with the analytic equation. One may expect that the inverse cascade of energy is the result of small scale instabilities that grow and finally saturate. Mathematically, these instabilities will be controlled by higher-order derivatives. We have performed numerical simulations of Burgers turbulence in which we turn off the nonoscillatory approximations in MDPATA in regions of expansion; the results have numerical oscillations, but are stable. Of course, when the full MPDATA is used, these oscillations are suppressed, possibly along with some of the physical variability as well. We believe that an optimal answer would lie between these two results.

Note that NFV schemes are not constructed with the purpose of zeroing the term $-u_xu_{xx}$ in expansion; rather this is a result of the upstream differencing. There is a strong connection [12] between the nonoscillatory property of NFV schemes and the second law of thermodynamics, which states that entropy must not decrease in a closed system. Consider now the finite volume energy equation associated with MPDATA and recall that in a Burgers fluid, the entropy is $-\bar{u}^2$. Thus another interpretation of the MPDATA energy equation is that entropy increases *locally in each cell*. However, an individual computational cell is not a closed system. Thus the MPDATA energy/entropy equation is a sufficient, but not necessary condition to enforce the second law. One might suppose that relaxing this local constraint, while enforcing the second law in a more global fashion, might achieve the more optimal result suggested in the previous paragraph.

How might one relax the nonoscillatory property? One strategy (at least conceptually) would be to enforce the second law on pairs of cells rather than on each cell individually. Clearly this would require expanding the stencil of the algorithm, and presumably altering the form of both the third-order and higher-order truncation terms. This approach is probably not practical, but suggests an alternative—to design an algorithm whose higher-order truncation terms also have some desired form. The construction of an algorithm from a desired form of a modified equation, a kind of reverse engineering, is one topic of our current research.

6. NUMERICAL EXPERIMENTS

In this section, we justify the use of the modified equation as a tool to understand the properties of MPDATA, and to investigate the sensitivity of the simulations to the dimensionless coefficients of the truncation error terms. We also compare several approaches to LES simulations of Burgers' equation.

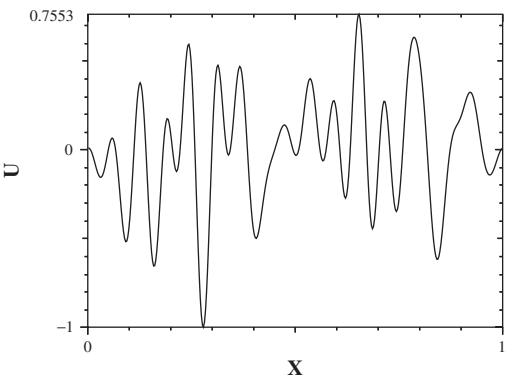

Figure 1. The initial condition for the multimode random *sine* wave for both the MPDATA and the DNS simulations.

6.1. Comparisons of MPDATA and its modified equation

Here we verify our hypothesis that the properties of MPDATA may be understood in terms of its modified equation. We will conduct numerical experiments where we solve and compare Burgers' equation using two methods: the MPDATA algorithm described in Section 2, and by direct numerical simulation of the MPDATA modified equation (8). For convenience we write a general equation in the form:

$$\begin{aligned}\bar{u}_t = &-\bar{u}\bar{u}_x + \lambda\bar{u}_{xx} + (\alpha\bar{u}_x\bar{u}_{xx} + \beta|\bar{u}_x|\bar{u}_{xx} + \xi\bar{u}\bar{u}_{xxx})(\delta x)^2 \\ &+ \gamma\bar{u}_{xxxx}(\delta x)^3 + (\eta\bar{u}_x^3/\bar{u})(\delta x)^2 \end{aligned} \tag{38}$$

This form will allow us to test the sensitivity of the modified equation and, once the correspondence is established, of MPDATA, to changes in the various coefficients. For basic MPDATA, we choose $\alpha = -\frac{1}{4}$, $\beta = \frac{1}{4}$, $\xi = -\frac{1}{6}$ and $\eta = 0$. We also use a coefficient $\gamma = -\frac{1}{6}$ to represent the higher-order dissipation. Note that we have ignored the Courant number (U) dependence in the coefficients.

We use a direct numerical simulation of the modified equation (DNS-ME) to accurately compute all the truncation terms. The DNS-ME program uses fourth-order centred differences and is integrated in time using the classic fourth-order Runge–Kutta method. In this case, DNS does not imply we are resolving the viscous length scales of the problem, but rather that we are simulating the modified equation of MPDATA accurately for a given choice of computational cell size and time step. Indeed, in these problems the DNS-ME method is unstable when only the basic Burgers' equation is simulated (i.e., $\alpha = \beta = \gamma = \xi = \eta = 0$). Our test problem is a multimode sine wave, with initial condition

$$u(x) = \sum_{m=1}^{20} a\sin(2m\pi(x-b)) \tag{39}$$

where a and b are random variables. The multimode initial condition is shown in Figure 1. Note that this problem contains many regions of both compression and expansion.

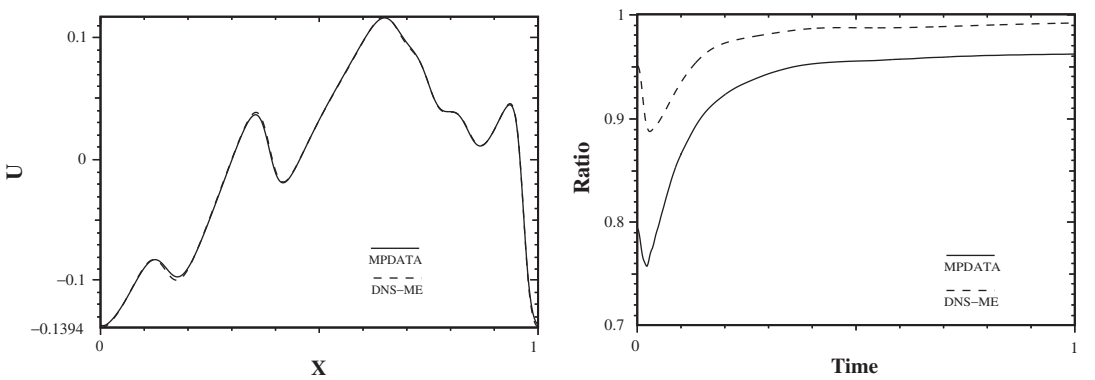

Figure 2. Comparing the final solutions for the multimode random *sine* wave using MPDATA and the DNS-ME for high viscosity $\lambda = 0.001$. The right figure compares the time histories of the ratio of the viscous and the total energy dissipation rates from MPDATA and the DNS-ME for high viscosity.

The MPDATA simulations use 400 cells over the interval $[0, 1]$, and a small time step, corresponding to a Courant number of 0.05, to minimize the effect of ignoring the Courant number dependence in the DNS-ME equations. We have run the DNS-ME model with increasing numbers of cells to insure numerical convergence. We consider two cases, one with the physical viscosity $\lambda = 0.001$ to represent large viscosity, and the other with $\lambda = 0.00001$ to represent low viscosity. By high (low), we mean that the term $\lambda \bar{u}_{xx}$ is comparable in size to (is much less than) $\bar{u}\bar{u}_x$, based on scale analysis.

We will use three bases of comparison between the MPDATA and the DNS-ME runs. First, we will plot the final solutions together for each case (at time $t = 1.0$). Second, we will compare the time history of the global kinetic energy. Third, we will compare the ratio of the rate of dissipation of kinetic energy by viscosity to the total rate of dissipation. This is computed by summing the viscous dissipation on the grid, $\lambda u u_{xx}$ and forming the ratio,

$$\frac{\sum_i \lambda u_i u_{xx,i}}{\sum_i \frac{1}{2}(u_i^2)_t} \tag{40}$$

The results for the high viscosity case are shown in Figures 2 and 4 (left panel). The comparison of the final solutions in Figure 2 is excellent, with tiny differences appearing only at the tops and bottoms of the shocks. We note that it is in these cells that $\bar{u}_x$ changes sign. As noted previously, in these cells MPDATA becomes only first-order accurate, and so is much more dissipative than DNS-ME. The comparison of the ratio of the energy dissipation rates and the energy histories (Figure 4) show similar close agreement.

The results for the low viscosity case are shown in Figures 3 and 4 (right panel). The solutions are sharper and steeper in this case. Nevertheless, the comparison of the final solutions and the ratio of viscous to total energy dissipation (Figure 3), and the energy dissipation history (Figure 4) all remain in excellent agreement. *These results support the proposition that the modified equation closely describes the properties of the MPDATA algorithm.*

Finally we describe two experiments with the DNS-ME model where we modify the coefficients of the truncation terms. For the coefficient ξ of the dispersive term $\bar{u}\bar{u}_{xxx}$, we found little sensitivity either to the sign of this term, or to doubling its magnitude. This is comforting,

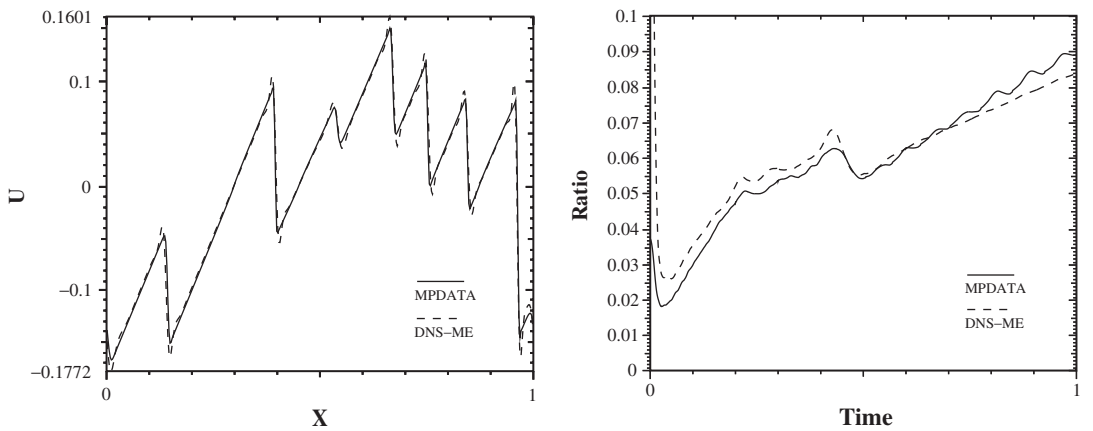

Figure 3. The final solution for the multimode random *sine* wave using MPDATA and the DNS-ME for low viscosity $\lambda = 0.00001$. The right figure compares the time histories of the ratio of the viscous and the total energy dissipation rates from MPDATA and the DNS-ME for low viscosity.

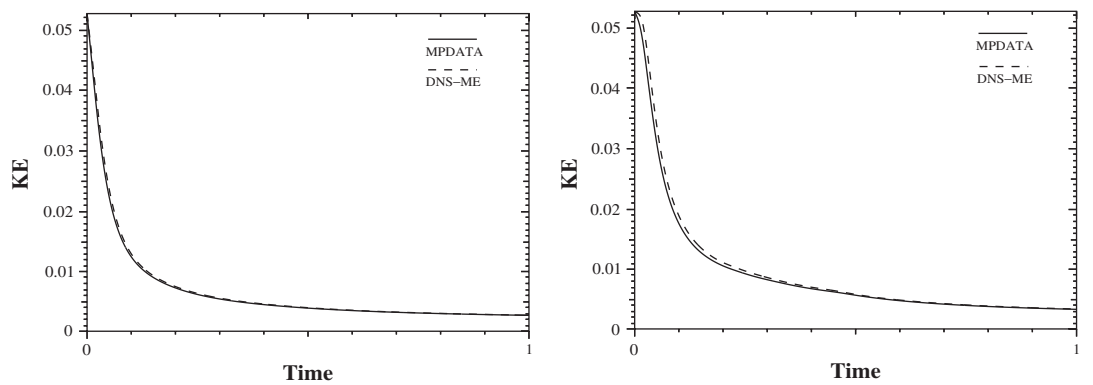

Figure 4. Comparing the kinetic energy histories for the high viscosity (left panel) and low viscosity (right panel) cases. The modified equation closely reproduces the MPDATA dissipation but is very slightly less dissipative.

for these terms have no analog in the analytic equations. We also note that it is possible to remove (i.e., compensate) these terms in MPDATA while maintaining its nonoscillatory character [5].

The results of experiments with the coefficient η of the nonlinear term $\bar{u}_x^3$ are more interesting. In principle, this term is closely related to the analytic result of Frisch—see Equation (11) in Section 3. In fact, this term is sufficient to stabilize the simulations with the coefficients of all other third-order terms set to zero. The value predicted by Frisch of $\eta = -\frac{1}{12}$ is large enough. However, we also note that these simulations are oscillatory and admit entropy violating rarefaction shocks.

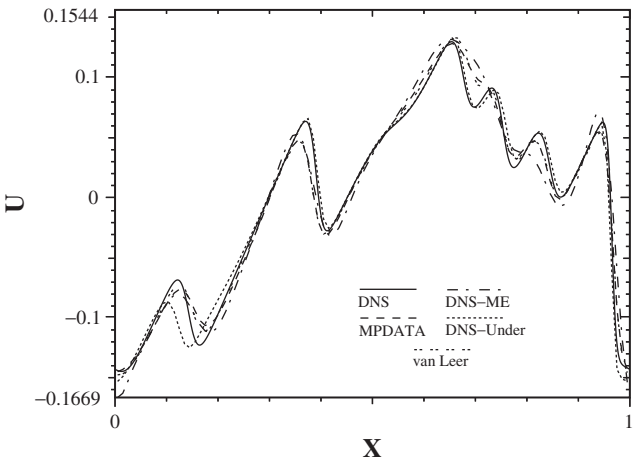

Figure 5. A comparison of the multimode solutions at $t = 1.0$ with a larger viscosity, $\lambda_1 = 0.0005$, for DNS and several LES alternatives.

6.2. *Large Eddy simulations*

Here we compare several approaches to LES modelling of our multimode problem of the previous section. Our purpose is to show that the NFV approach can give accurate results with reasonable computational effort, when compared with DNS simulations of Burgers' equation and with our DNS-ME simulations of the MPDATA modified equations. We will not compare the NFV approach to any of the many explicit turbulence models for LES; this represents an important effort for the future, but lies outside the scope of the present work.

In particular, we will compare five approaches: (1) a DNS simulation (by which we mean the resolution is sufficient that the physical viscosity is responsible for essentially all of the energy dissipation; (2) an underresolved DNS, which uses the same DNS algorithm but with much lower resolution; (3) MPDATA at the same lower resolution; (4) DNS-ME of the MPDATA modified equation at the same lower resolution; (5) a standard van Leer algorithm at the same lower resolution. The purpose of including the van Leer algorithm, which is an alternate NFV scheme based on geometric flux limiting [18], is to reinforce our contention that it is the NFV properties in general, rather than MDPATA in particular, which is responsible for the implicit turbulence modelling. A unified discussion of nonoscillatory schemes based on flux limiting can be found in Reference [19].

We use two versions of our multimode problem, both with the same initial conditions given by Equation (39), but employing two different values of the viscous coefficients—$\lambda_1 = 0.0005$ and $\lambda_2 = 0.0002$. The DNS simulation of Burgers' equation (7) using 800 cells is well-resolved for both viscosities and represents 'truth' for purposes of comparison. We repeat these runs using 100 cells in each of our four LES approaches.

For the higher viscosity λ_1, the five solutions are plotted together in Figure 5. Here the underresolved DNS is generally closest to the DNS, although it is on the edge of numerical stability in the early stages of the simulation when the shocks are forming. The MPDATA and van Leer runs are nearly identical. Both reproduce the large scale features of the solution. Both exhibit small discrepancies in the positions of a few of the shock peaks and minima,

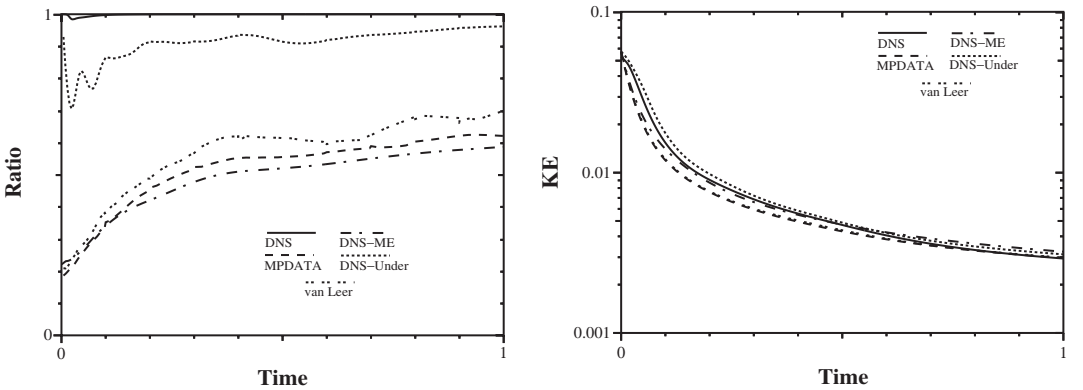

Figure 6. A comparison of the multimode solution's kinetic energy decay with a larger viscosity, $\lambda_1 = 0.0005$, for DNS and several LES alternatives.

likely associated with the unphysical dispersive terms that appear among the truncation error. The DNS-ME run is the least accurate. Although DNS-ME and MPDATA exhibit close agreement in experiments in the previous subsection (cf. Figures 2 and 3), the coarser resolution employed here (100 cells versus 400 cells) degrades this agreement.

The kinetic energy dissipation history in Figure 6 (left panel) shows that in the underresolved DNS run about 90 per cent of the energy dissipation is viscid (i.e., is dissipated by the physical viscosity). This is presumably the reason that this simulation does well—i.e., this run is 'nearly' DNS. By contrast in the MPDATA, DNS-ME and van Leer runs, nearly half the energy is dissipated by the inviscid terms (i.e., by the numerical method). The kinetic energy history is shown in Figure 6 (right panel). Each of the LES runs does well in this comparison, though all are more dissipative than the DNS in the early stages of shock formation.

The four solutions for the lower viscosity case λ_2 are shown in Figure 7. Although λ_2 is only slightly smaller than λ_1, the underresolved DNS has become unstable. The MPDATA and van Leer runs are again in excellent agreement with each other, and faithfully reproduce the resolved scales of the DNS simulation. As in the previous case, the DNS-ME run is the least accurate.

The kinetic energy dissipation history is shown in Figure 8 (left panel). Here even the DNS run has some inviscid dissipation in its early stages. All the LES runs are dominated by the inviscid dissipation (the underresolved DNS run was not stable). The right panel of this figure shows the kinetic energy history. Again all LES runs compare well with the DNS run.

To summarize, the two NFV simulations are very similar to each other and are the most computationally efficient. Both MPDATA and the van Leer simulations produce high quality solutions on coarse grids, using a relatively small number of comparisons. For example, the MPDATA simulation using 100 cells requires only 70 time steps while the DNS simulation using 800 cells requires 1700 time steps. In terms of function evaluations, the MPDATA run is about 400 times less expensive, illustrating the value of the LES approach.

Finally, we note a less quantifiable though nevertheless important feature of the NFV simulations, namely robustness. When the simulated flow becomes too variable to represent on the grid (for example in the process of shock formation), NFV algorithms add dissipation

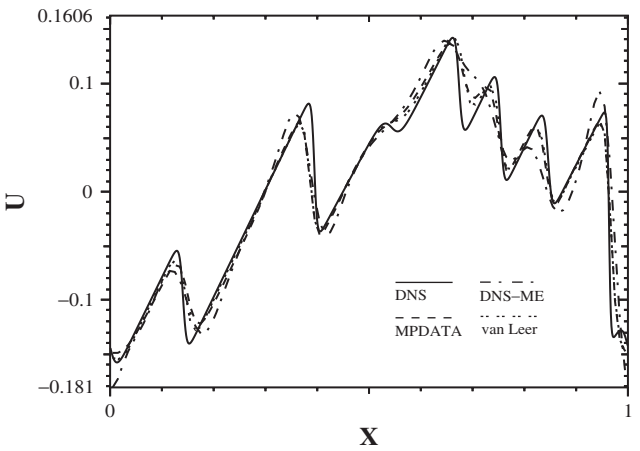

Figure 7. A comparison of the multimode solutions at $t = 1.0$ with a larger viscosity, $\lambda_2 = 0.0002$, for DNS and several LES alternatives.

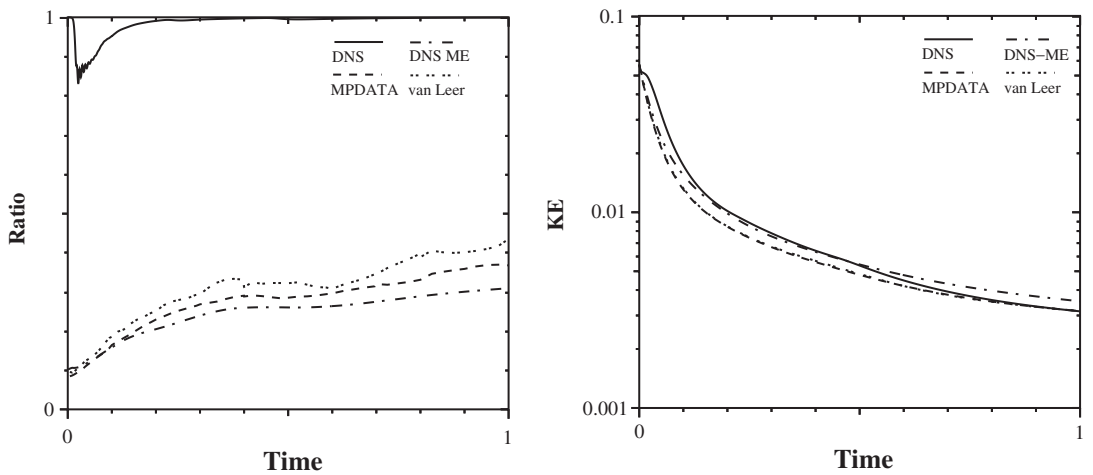

Figure 8. A comparison of the multimode solution's kinetic energy decay with a larger viscosity, $\lambda_2 = 0.0002$, for DNS and several LES alternatives.

selectively to maintain smooth and reasonable solutions. This point is illustrated in Figures 2 and 3 by the lack of oscillations at the velocity maxima and minima.

7. DISCUSSION

In this paper, we have attempted to provide a rationale for the success of nonoscillatory finite volume (NFV) schemes to represent turbulent flow with significant unresolved scales without recourse to a subgrid scale model—a property we have termed implicit turbulence modelling.

Our strategy has been to demonstrate that the truncation errors of these methods, as determined by comparison with the point equations that govern the fluid flow, have physical significance, and indeed are the corrections necessary to represent the evolution of a finite volume of fluid.

Our principal results are in Section 4 and pertain to a one-dimensional fluid governed by Burgers' equation. When the flow is smooth over some scales of length and time, we expanded the velocity in a Taylor series and averaged the equations over those length and time scales. This led to several new terms that scaled with the square of the space or of the time intervals. For flows that are not laminar, i.e., for which the fluid velocity is not smooth over particular length and time scales, we made an additional assumption that averaged velocity at least is smooth over these scales. With this assumption, we were able to show that same averaged equations that govern the evolution of laminar flows also govern turbulent flows.

We believe this result is important both philosophically and practically. From the philosophical point of view, it means that the modeller does not have to know *a priori* whether a flow is turbulent. From the practical point of view, the same numerical models can be applied to laminar and to turbulent flow. Further, in physical terms our assumption about smoothness implies only that the flow can in fact be modelled by discretized PDEs, an assumption that is usually made implicitly in the application of a model.

In closing this paper, it is appropriate to note some limitations and to suggest directions for continuing research. First of all, we have focused on one-dimensional Burgers' equation, but are ultimately interested in the multidimensional Navier–Stokes equations. Second, one may expect that the analytic derivations will not hold near a wall when the boundary layer is not resolved. Third, the issues raised in Section 5 concerning variability and the ability of the algorithm to 'backscatter' small scale energy into the resolved flow need to be addressed.

Despite the work that remains to be done, we believe that the implicit turbulence modelling property of NFV schemes represents a useful research direction and an important simplification to the problem of numerically simulating turbulent flows. It appears that the reluctance of the community in general to accept implicit turbulence modelling is more due to the lack of justification of the approach rather than any failure of application. We offer this paper in the spirit of providing a first level of justification.

ACKNOWLEDGEMENTS

The authors acknowledge many interesting discussions with Darryl Holm and Piotr Smolarkiewicz. We have also benefited from discussions with J. A. Domaradzki, J. R. Kamm, R. B. Lowrie, J. R. Ristorcelli and E. S. Titi. LGM thanks the DOE Climate Change Prediction Program (CCPP) and DOE Applied Mathematics Program (MICS) for partial support of this work. WJR thanks the DOE Advanced Strategic Computing Initiative (ASCI) and the LANL Laboratory Directed Research and Development (LDRD) program. This work was performed under the auspices of the US Department of Energy under contract W-7405-ENG-36.

REFERENCES

1. Margolin LG, Smolarkiewicz PK, Sorbjan Z. Large eddy simulations of convective boundary layers using nonoscillatory differencing. *Physica D* 1999; **133**:390–397.
2. Oran ES, Boris JP. Computing turbulent shear flows—a convenient conspiracy. *Computers in Physics* 1993; **7**:523–533.
3. Porter DH, Pouquet A, Woodward PR. Kolmogorov-like spectra in decaying three-dimensional supersonic flows. *Physics of Fluids* 1994; **6**:2133–2142.

4. Smolarkiewicz PK, Margolin LG. MPDATA: a finite difference solver for geophysical flows. *Journal of Computational Physics* 1998; **140**:459–480.
5. Margolin LG, Smolarkiewicz PK. Antidiffusive velocities for multipass donor cell advection. *SIAM Journal of Scientific Computing* 1998; **20**:907–929.
6. von Neumann J, Richtmyer RD. A method for the numerical calculation of hydrodynamic shocks. *Journal of Applied Physics* 1950; **21**:232–237.
7. Smagorinsky J. General circulation experiments with the primitive equations. I. the basic experiment. *Monthly Weather Review* 1963; **101**:99–164.
8. Leonard A. Large-eddy simulation of chaotic convection and beyond. AIAA paper No. 97-0204, 1997.
9. Winkelmans GS, Wray AA, Vasilyev OV, Jeanmart H. Explicit-filtering large-eddy simulation using the tensor-diffusivity model supplemented by a dynamic Smagorinsky term. *Physics of Fluids* 2001; **13**:1385–1403.
10. Chen S, Foias C, Holm DD, Olson E, Titi ES, Wynne S. The Camassa–Holm equations as a closure model for turbulent channel and pipe flow. *Physics Review Letters* 1998; **81**:5538–5541.
11. Chen S, Holm DD, Margolin LG, Zhang R. Direct numerical simulations of the Navier–Stokes alpha model. *Physica D* 1999; **133**:66–83.
12. Merriam ML. Smoothing and the second law. *Computer Methods in Applied Mechanical Engineering* 1987; **64**:177–193.
13. Bethe H. On the theory of shock waves for an arbitrary equation of state. Technical Report NDRC-B-237, Office of Scientific Research and Development (1942). Reprinted in *Classic Papers in Shock Compression Science*. Springer-Verlag, 1998.
14. Kolmogorov AN. A refinement of previous hypothesis concerning the local structure of turbulence in viscous incompressible fluid at high Reynolds number. *Journal of Fluid Mechanics* 1962; **13**:82–85.
15. Frisch U. *Turbulence*: *the Legacy of A.N. Kolmogorov*. Cambridge University Press, 1995.
16. Smagorinsky J. The Beginnings of Numerical Weather Prediction and General Circulation Modeling: Early Recollections. *Advances in Geophysics* 1983; **25**:3–37.
17. Smagorinsky J. Some historical remarks on the use of nonlinear viscosities. *Large Eddy Simulation of Complex Engineering and Geophysical Flows*. Cambridge University Press, 1993, 3–36.
18. van Leer B. Toward the ultimate conservative difference scheme IV: A new approach to numerical convection. *Journal of Computational Physics* 1977; **23**:276–299.
19. Sweby PK. High resolution schemes using flux limiters for hyperbolic conservation laws. *SIAM Journal of Numerical Analysis* 1984; **210**:995–1010.